Visual–motor deficits relate to altered gray and white matter in young adults born preterm with very low birth weight

CrossMark

Kam Sripada [a,*], Gro C. Løhaugen [a,b], Live Eikenes [c], Kjerstin M. Bjørlykke [d], Asta K. Håberg [e], Jon Skranes [a,b], Lars M. Rimol [a]

[a] Department of Laboratory Medicine, Children's and Women's Health, Norwegian University of Science and Technology, Trondheim, Norway
[b] Department of Pediatrics, Sørlandet Hospital, Arendal, Norway
[c] Department of Circulation and Medical Imaging, Norwegian University of Science and Technology, Trondheim, Norway
[d] Akershus University Hospital, Medical Division, Oslo, Norway
[e] Department of Neuroscience, Faculty of Medicine, Norwegian University of Science and Technology, Trondheim, Norway

ARTICLE INFO

ABSTRACT

Individuals born preterm and at very low birth weight (birth weight $\leq$ 1500 g) are at an increased risk of perinatal brain injury and neurodevelopmental deficits over the long term. This study examined whether this clinical group has more problems with visual–motor integration, motor coordination, and visual perception compared to term-born controls, and related these findings to cortical surface area and thickness and white matter fractional anisotropy. Forty-seven preterm-born very low birth weight individuals and 56 term-born controls were examined at 18–22 years of age with a combined cognitive, morphometric MRI, and diffusion tensor imaging evaluation in Trondheim, Norway. Visual–motor skills were evaluated with the Beery–Buktenica Developmental Test of Visual–Motor Integration—V (VMI) copying test and its supplemental tests of motor coordination and visual perception. 3D T_1-weighted MPRAGE images and diffusion tensor imaging were done at 1.5 T. Cortical reconstruction generated in FreeSurfer and voxelwise maps of fractional anisotropy calculated with Tract-Based Spatial Statistics were used to explore the relationship between MRI findings and cognitive results. Very low birth weight individuals had significantly lower scores on the copying and motor coordination tests compared with controls. In the very low birth weight group, VMI scores showed significant positive relationships with cortical surface area in widespread regions, with reductions of the superior temporal gyrus, insula, and medial occipital lobe in conjunction with the posterior ventral temporal lobe. Visual perception scores also showed positive relationships with cortical thickness in the very low birth weight group, primarily in the lateral occipito-temporo-parietal junction, the superior temporal gyrus, insula, and superior parietal regions. In the very low birth weight group, visual–motor performance correlated positively with fractional anisotropy especially in the corpus callosum, inferior fronto-occipital fasciculus bilaterally, and anterior thalamic radiation bilaterally, driven primarily by an increase in radial diffusivity. VMI scores did not demonstrate a significant relationship to cortical surface area, cortical thickness, or diffusion measures in the control group. Our results indicate that visual–motor integration problems persist into adulthood for very low birth weight individuals, which may be due to structural alterations in several specific gray–white matter networks. Visual–motor deficits appear related to reduced surface area of motor and visual cortices and disturbed connectivity in long association tracts containing visual and motor information. We conjecture that these outcomes may be due to perinatal brain injury or aberrant cortical development secondary to injury or due to very preterm birth.

Introduction

Though their survival rates have risen greatly in recent decades, individuals born preterm with very low birth weight (VLBW: birth weight $\leq$ 1500 g) are at an increased risk of perinatal brain injury, including focal and diffuse periventricular leukomalacia (Volpe, 2001), and neurodevelopmental deficits over the long term (Aarnoudse-Moens et al., 2009). While the behavioral and cognitive outcomes of preterm birth and VLBW have been well-documented, the patterns of neurodevelopmental changes in both gray and white matter underlying visual–motor performance in young adulthood remain an open question.

Periventricular leukomalacia is strongly associated with motor problems, such as cerebral palsy, cognitive deficits, and perceptual impairments, and periventricular deep white matter damage can affect

* Corresponding author at: Department of Laboratory Medicine, Children's and Women's Health, Medical Faculty, Norwegian University of Science and Technology, 7489 Trondheim, Norway.
E-mail address: kam.sripada@ntnu.no (K. Sripada).

projection fibers, such as the corticospinal tract, and association fibers including the long association tracts and the optic radiations (Staudt et al., 2003; Krageloh-Mann et al., 1999; van den Hout et al., 2004; Platt et al., 2007; Sullivan and Margaret, 2003; Evensen et al., 2004; Davis et al., 2005; Hard et al., 2000; McGrath and Sullivan, 2002). Visual–motor function includes multiple components: visual perception, eye-hand coordination, fine motor skills and speed, and visual–motor integration (Aylward, 2005). Thus, assessment of visual–motor function is complex, and poor visual–motor performance may reflect deficits associated with one of these components alone or a combination. The latter has been reported for preterm-born children (Evensen et al., 2009). Poorer visual function, including reduced visual acuity and visual–motor problems, has been reported to be more prevalent among VLBW children and adolescents (Lindqvist et al., 2007, 2008; Hellgren et al., 2007; Goyen et al., 1998). Moreover, preterm-born children are at risk for developing motor function deficits and have demonstrated significantly higher rates of motor impairment compared to controls (Spittle et al., 2011; Williams et al., 2010).

Morphometric magnetic resonance imaging (MRI) and diffusion tensor imaging (DTI) sequences are sensitive to distinct but complementary layers of structural organization, and by combining them it is possible to paint a more detailed picture of brain development (Dubois et al., 2014). Cortical surface area and thickness analyses are seen as increasingly important datapoints in clinical MR research for characterizing gray matter (Panizzon et al., 2009). By contrast, DTI makes possible the study of microstructural changes and white matter connectivity and is one of few approaches available today to trace white matter connectivity in vivo non-invasively in the human brain (Le Bihan and Johansen-Berg, 2012). Brownian motion of water molecules in the brain is hindered by cell membranes, and diffusion MRI can indicate the axial and radial diffusivity of water along white matter fiber bundles (Johansen-Berg and Behrens, 2009; Vasung et al., 2013).

Morphometric MRI techniques have yielded insights about gray matter alterations related to preterm birth (Lax et al., 2013), and likewise DTI has demonstrated microstructural differences in the brains of VLBW and term-born children and the persistence of these effects through childhood and into early and late adolescence (Ment et al., 2009; Mento and Bisiacchi, 2012; Skranes et al., 2007; Eikenes et al., 2011). In a recent study, Kim et al. (2014) combined graph theory analysis and DTI tractography and reported that longer gestational periods in typically developing children enhanced efficiency of both local and global structural brain networks. However, little neuroimaging research employing both morphometric and DTI data in the preterm-born population has focused on on visual–motor function (Tao and Neil, 2014).

MRI research has identified sequelae of preterm birth and VLBW, ranging from reductions in white matter, gray matter, and overall brain volume in childhood and adolescence (de Kieviet et al., 2012; Giménez et al., 2004) to brain correlates of behavioral problems, such as inattention and hyperactivity in childhood (Bora et al., 2014) and socialization problems in adolescence (Healy et al., 2013). Diverse cortical and subcortical structures have been implicated in patterns of altered brain development following preterm birth. Previous long-term follow-up studies comparing VLBW and term-born individuals have demonstrated alterations in gray matter structure, including reductions in cortical surface area in ventrolateral prefrontal, temporal and parietal regions in VLBW individuals by age 19 (Skranes et al., 2013), differential patterns of cortical thickness between VLBW and controls by early adulthood (Bjuland et al., 2013), and regions of increased and decreased structural covariance between the groups by adolescence (Nosarti et al., 2011).

White matter studies with VLBW individuals have identified reduced posterior corpus callosum surface area (Nosarti et al., 2004), lower FA in bilateral uncinate fasciculi (Mullen et al., 2011), external capsules, corpus callosum splenium (Constable et al., 2008; Vangberg et al., 2006; Eikenes et al., 2011), and other intrahemispheric association fibers. A smaller subset of these have begun to identify associations between specific white matter tract alterations and diverse cognitive functions, such as language processing (Reidy et al., 2013; Mullen et al., 2011), IQ (Iwata et al., 2012), and perceptual and motor functions (Skranes et al., 2007; Chau et al., 2013).

Previous reports on this cohort (Eikenes et al., 2011; Skranes et al., 2007, 2013; Bjuland et al., 2013, 2014; Lindqvist et al., 2011; Vangberg et al., 2006) have documented alterations in gray and white matter structures in VLBW individuals. The current study expands on these by investigating MRI data in the context of visual–motor integration at entry to adulthood and assessing specific cortical regions and white matter structures that may be sensitive to VLBW.

Aim

This study assesses visual–motor function in the context of brain development by combining cognitive assessment with structural MRI and DTI. The first aim of this study was to evaluate visual–motor abilities for copying figures, fine motor tasks, and visual perception in young adults born with VLBW compared to age-equivalent term-born controls. The second aim was to relate visual–motor and visual–perceptual abilities in the VLBW group to morphometric and DTI findings. Our hypothesis was that the VLBW adults would achieve lower scores than controls on these visual–motor tests and demonstrate corresponding gray and white matter alterations.

Methods

Study design

This study is part of a hospital-based prospective follow-up study of three year cohorts of children. A total of 121 VLBW infants were admitted to the neonatal intensive care unit (NICU) at the university hospital in Trondheim, Norway, between 1986 and 1988. The control infants were born to mothers living in the Trondheim area and were enrolled in a multi-center study before week 20 of pregnancy, between January 1986 and March 1988. All the births in a 10% random sample of mothers (paras 1 and 2) were included for follow-up during pregnancy. Neuroimaging and cognitive data collection for the present study was carried out between January 2007 and December 2008.

Study population

VLBW group

Of the 121 VLBW infants admitted to the NICU, 33 died, and nine had moved before follow-up. One child with Down's syndrome and two children with severe cerebral palsy were excluded from follow-up due to inability to perform the tests. Of the remaining 76, 54 (71%) participated in follow-up evaluation at age 18–22, and 47 (61%), including 3 individuals with mild bilateral spastic cerebral palsy, had successful cognitive assessments and MRI acquisitions. Twelve of the VLBW participants were twins.

Control group

The control group comprised 120 infants from the 10% random sample born at term, with birth weight ≥ 10th percentile for gestational age. At age 18–22, 10 had moved and two were excluded due to congenital malformations. Of the remaining 108, 81 (75%) participated at the follow-up, and 66 were examined with MRI. Seven DTI scans were excluded due to image artifacts, leaving 59 with successful DTI scans. Three of these did not have VMI assessment or had a poor morphometric MRI, leaving 56 (52%) who were successfully evaluated with cognitive testing, morphometric MR, and DTI.

MRI acquisition

MRI data were acquired on a 1.5 T Siemens Magnetom Symphony (Siemens, Erlangen, Germany) with Quantum gradients (30 mT/m) and a quadrature head coil. A structural T_1-weighted magnetization prepared rapid acquisition gradient echo (MPRAGE) sequence was acquired with TR = 7.1 ms, TE = 3.45 ms, TI = 1000 ms, flip angle 7°, FOV 256 × 256, slab thickness 170 mm, and acquisition matrix 256 × 192 × 128, reconstructed to 256 × 256 × 128, giving a reconstructed voxel resolution of 1 × 1 × 1.33 mm. The DTI sequence was a single-shot balanced-echo EPI sequence acquired in 12 non-collinear directions with b = 1000 s/mm² using the following parameters: TR = 10,400 ms, TE = 100 ms, FOV 280 × 280 mm, slice thickness 2.2 mm, and acquisition matrix 128 × 128, giving isotropic voxels of 2.2 mm. Fifty-five transversal slices with no gap were acquired, giving full brain coverage. The slices were obtained parallel to the anterior/posterior commissural line. For each slice, two images without diffusion weighting (b = 0), and 12 images with diffusion gradients were acquired. The DTI sequence was repeated six times for an increased signal-to-noise ratio.

Morphometric image analysis

The MPRAGE images were reviewed for image quality, and low quality images were excluded. The quality of the FreeSurfer image processing was reviewed by image analyzers blinded to group adherence, in order to check the quality of the cortical reconstruction and apply minimal manual editing in a few cases.

Cortical reconstruction for cortical thickness and surface area measurements was performed with the FreeSurfer 5.1.0 image analysis suite (http://surfer.nmr.mgh.harvard.edu). The technical details of these procedures are described in prior publications (Dale et al., 1999; Dale and Sereno, 1993; Fischl and Dale, 2000; Fischl et al., 1999a,b, 2001, 2002, 2004a,b; Han et al., 2006; Jovicich et al., 2006; Ségonne et al., 2004). Briefly, this processing includes motion correction and averaging (Reuter et al., 2010) of multiple volumetric T_1-weighted images, removal of non-brain tissue using a hybrid watershed/surface deformation procedure (Ségonne et al., 2004), automated Talairach transformation, intensity normalization (Sled et al., 1998), tessellation of the gray and white matter boundary, automated topology correction (Fischl et al., 2001; Ségonne et al., 2007), and surface deformation following intensity gradients to optimally place the gray/white and gray/cerebrospinal fluid (CSF) borders at the location where the greatest shift in intensity defines the transition to the other tissue class (Dale et al., 1999; Dale and Sereno, 1993; Fischl and Dale, 2000). Once the cortical models are complete, a number of deformable procedures can be performed for further data processing and analysis including surface inflation (Fischl et al., 1999a), registration to a spherical atlas which is based on individual cortical folding patterns to match cortical geometry across individuals (Fischl et al., 1999b), parcellation of the cerebral cortex into units with respect to gyral and sulcal structure (Desikan et al., 2006; Fischl et al., 2004b), and creation of a variety of surface-based data. This method uses both intensity and continuity information from the entire three-dimensional MR volume in segmentation and deformation procedures to produce representations of cortical thickness, calculated as the closest distance from the gray/white boundary to the gray/CSF boundary at each vertex on the tessellated surface (Fischl and Dale, 2000). The maps are created using spatial intensity gradients across tissue classes and are therefore not simply reliant on absolute signal intensity.

The two cerebral hemispheres were processed separately. The surfaces were smoothed with a full-width-half-maximum Gaussian kernel of 30 mm (662 iterations) and averaged across participants. Each surface consisted of 163,842 vertices arranged in a triangular grid, and estimates of cortical area were obtained by computing the area of each triangle in the standardized, spherical atlas space surface tessellation when mapped into the individual subject space. Vertex-wise estimates of relative areal expansion for each individual in atlas space were then computed by assigning one-third of the area of each triangle to each of its vertices (Rimol et al., 2012). The cortical surface for each individual was automatically parcellated using defined gyri and sulci as landmarks, and the surface was divided into 34 anatomical regions for each brain hemisphere defined in FreeSurfer (Fischl et al., 2004b; Desikan et al., 2006), which were used to anatomically identify affected regions after significance testing.

Morphometry statistical analysis

All statistical analyses of morphometry data were performed within the MATLAB software suite 2011b (MATLAB and Statistics Toolbox Release 2011b. The MathWorks, Inc., Natick, Massachusetts, US). A general linear model was fitted in each of the 163,842 vertices per cerebral hemisphere, with cortical surface area or cortical thickness as dependent variable, and adjusted for sex and age at MRI, with one of the VMI tests (copying, motor, or visual) as continuous predictor. The appropriate contrast vectors were set to test for a relationship between performance on each of the VMI tests and cortical morphology. The hemispheres were analyzed separately, and effect size and p-maps were generated. Effect size was obtained as explained variance ($r^2 = (F / (f + df))$). To correct for multiple comparisons, the two p-maps from left and right hemisphere were combined and thresholded to yield an expected false discovery rate (FDR) of 5% across both hemispheres.

DTI analysis

DTI analysis was performed with the FMRIB software library (FSL, Oxford Centre for Functional MRI of the Brain, Oxford, UK; www.fmrib.ox.ac.uk/fsl). All DTI acquisitions were registered to the b = 0 image using affine registration in order to minimize image artifacts caused by motion and eddy current distortions. FMRIB's Diffusion Toolbox was used to fit a diffusion tensor model to the raw diffusion data in each voxel (Basser and Pierpaoli, 1996) and create voxelwise maps of the eigenvalues (λ_1, λ_2, and λ_3), FA, and mean diffusivity (MD) for both the VLBW and control groups.

FSL's Tract-Based Spatial Statistics (TBSS) (Smith et al., 2006) was used for voxel-based analysis of the DTI data. Randomise was used to study the relationship between the skeletonized FA, MD, and eigenvalues (λ_1, λ_2, and λ_3) and scores on the three VMI tests (copying, motor, and visual) in the VLBW and control groups separately. Randomise performs nonparametric permutation tests with a correction for multiple comparisons, here corrected for sex and age at MRI ($p < 0.05$) (Nichols and Holmes, 2002). Anatomical locations were identified using the Johns Hopkins University International Consortium of Brain Mapping-DTI-81 White-Matter Labels and Johns Hopkins University White-Matter Tractography atlases within FSL (Wakana et al., 2007; Hua et al., 2008) and human white matter atlases by Oishi et al. (2011) and Mori et al. (2005).

Visual–motor integration evaluation

Visual–motor integration was assessed with the Beery–Buktenica Developmental Test of Visual–Motor Integration—V (VMI) and its two supplemental tests. VMI is a widely used standardized test that requires both motor and perceptual skills (Beery et al., 2004). In the copying test (hereafter referred to as "copying"), the participant is instructed to copy 30 geometric designs in increasing order of difficulty without a time limit. The designs are scored according to the VMI manual based on accuracy and quality standards. If the participant fails to copy three consecutive designs, the test may be stopped. The first supplemental test, visual perception ("visual"), requires the participant to match visual shapes within a 3-minute time limit. Total number of correctly

matched designs is the raw score. The second supplemental test, motor coordination ("motor"), requires the participant to trace the designs with a pencil without leaving the double-lined paths in which the designs are presented, within 5 min. For the supplemental tests, the participants are allowed to continue throughout the time allotted, regardless of failed tasks. Thirty points is the maximum raw score for each of the three tests.

Cognitive data analysis

The software package IBM SPSS 21 (Chicago, USA) was used for statistical analysis of the cognitive data. Differences between groups in age at exam, socioeconomic status, and maternal age at childbirth were investigated with t-tests, and effect of twin status on VMI scores was assessed with univariate ANOVA. A general linear model with age at MRI, sex, and socioeconomic status as covariates was used for analysis of the three VMI tests. Demographic and clinical data are presented in Table 1.

Socioeconomic status

Socioeconomic status was calculated using Hollingshead's two factor index of social position based on education and occupation of one parent or the mean index of both parents (Hollingshead, 1957).

Ethics

Written, informed consent was obtained from the participating young adults, and the Data Inspectorate assigned the license for keeping a data register with personal information. The Regional Committee for Medical Research Ethics approved the study protocol (project number: 4.2005.2605).

Results

Group characteristics

Demographic and clinical characteristics of the study groups are shown in Table 1. Birth weight and gestational age were selection criteria for the two groups. In the VLBW group, mean birth weight was 1221 g and mean gestational age was 29.3 weeks. There was no difference in age at exam (p = 0.90), socioeconomic status (p = 0.12), or maternal age at childbirth (p = 0.08) between the groups.

Cognitive test results and group differences

The VLBW group had lower scores than controls on the copying and motor tests but not on the visual test after adjusting for age, sex, and socioeconomic status. Raw scores for the three VMI tests are presented with age, sex, and socioeconomic status as covariates in a general linear model in Table 2. The univariate ANOVA yielded no significant effect of twin status on VMI scores.

Table 1
Demographic and clinical information. Mean values ± standard deviation, [95% confidence intervals].

Characteristics	VLBW (n = 47)	Control (n = 56)
Birth weight (g)	1221 ± 231, [1153, 1289]	3694 ± 495, [3561, 3826]
Gestational age (weeks)	29.3 ± 2.5, [28.5,30.0]	39.8 ± 1.3, [39.4,40.1]
Sex (male/female)	20/27	21/35
Age at exam (years)	19.7 ± .9	19.7 ± .6
Socioeconomic status (1–5)	3.4 ± 1.3, [3.0,3.8]	3.8 ± .88, [3.5,4.0]
Maternal age (years)	29.0 ± 4.7, [27.6,30.3]	30.5 ± 3.9, [29.4,31.5]

Abbreviations: VLBW, very low birth weight.

Table 2
Results of the three VMI tests in the two study groups. Mean raw scores ± standard deviation, [95% confidence intervals].

VMI assessment	VLBW (n = 47)	Control (n = 56)	p-value
Copying	24.6 ± 3.6, [23.7, 25.4]	26.7 ± 2.4, [25.9, 27.5]	.001
Motor	27.4 ± 2.7, [26.8, 28.1]	29.2 ± 1.8, [28.6, 29.8]	<.001
Visual	27.6 ± 2.0, [27.0, 28.3]	27.9 ± 2.3, [27.3, 28.4]	.609

Abbreviations: VLBW: very low birth weight; VMI: Beery–Buktenica Developmental Test of Visual–Motor Integration−V.

Structural MRI

Cortical surface area

In the VLBW group, there were widespread cortical regions in both hemispheres showing a significant relationship between each of the three VMI tests and cortical surface area. Table 3 lists all regions with significant findings in the VLBW group as determined by the general linear model (after FDR correction), with several regions significant across the VMI tests (Fig. 1). The explained variance reached 35–40% in several highly correlated regions (yellow in Fig. 2) and was as high as 48% in the right lingual and lateral occipital gyri for the copying test. Explained

Table 3
Proportion (%) of surface area in cortical regions of interest showing significant relationship with VMI tests (copying, motor, visual) in the VLBW cohort.

Cortical region of interest	Copying		Motor		Visual	
	Left	Right	Left	Right	Left	Right
Banks of the superior temporal gyrus	68	70	100	77	77	82
Caudal anterior cingulate gyrus	0	8	22	100	79	81
Caudal middle frontal gyrus	36	20	95	64	58	54
Cuneus	100	31	100	48	100	63
Entorhinal cortex	0	0	2	0	100	0
Fusiform gyrus	63	47	95	74	96	78
Inferior parietal gyrus	30	34	52	80	57	70
Inferior temporal gyrus	11	4	51	38	41	25
Insula	94	99	67	100	100	99
Isthmus cingulate	44	42	42	63	63	100
Lateral occipital gyrus	74	51	96	85	88	98
Lateral orbitofrontal gyrus	73	73	85	100	100	96
Lingual gyrus	100	100	100	94	100	100
Medial orbitofrontal gyrus	17	44	100	86	100	93
Middle temporal gyrus	48	25	59	83	82	31
Parahippocampal gyrus	76	69	68	76	100	90
Paracentral gyrus	7	13	90	76	22	34
Pars opercularis	76	28	100	83	100	41
Pars orbitalis	0	100	100	100	100	100
Pars triangularis	1	74	95	100	100	77
Pericalcarine sulcus	100	84	100	79	100	100
Postcentral gyrus	9	13	21	19	14	16
Posterior cingulate	32	88	71	100	84	97
Precentral gyrus	40	21	58	73	55	34
Precuneus	41	47	70	54	43	62
Rostral anterior cingulate	0	46	82	100	95	100
Rostral middle frontal gyrus	49	55	100	81	95	83
Superior frontal gyrus	69	47	98	87	94	91
Superior parietal gyrus	32	38	61	88	38	44
Superior temporal gyrus	85	86	92	99	83	100
Supramarginal gyrus	1	8	38	12	8	39
Frontal pole	33	0	100	41	100	100
Temporal pole	25	4	93	76	100	57
Transverse temporal gyrus (Heschl's gyrus)	100	100	100	100	100	100

The table presents the percentage of surface area in each of the parcellations (from the FreeSurfer Desikan–Killiany parcellation scheme) that showed a significant result (after FDR correction) in the GLM testing for a relationship between the VMI tests and cortical surface area in the VLBW cohort. The GLMs were fitted with cortical surface area as dependent variable, sex as categorical predictor, and age at MRI scan and one of the VMI test scores as continuous predictors. Contrast vectors were set to test for a relationship between performance on each of the VMI tests (copying, motor, visual) and cortical surface area.
Abbreviations: FDR, false discovery rate; GLM, general linear model; VLBW, very low birth weight; VMI, Beery–Buktenica Developmental Test of Visual–Motor Integration−V.
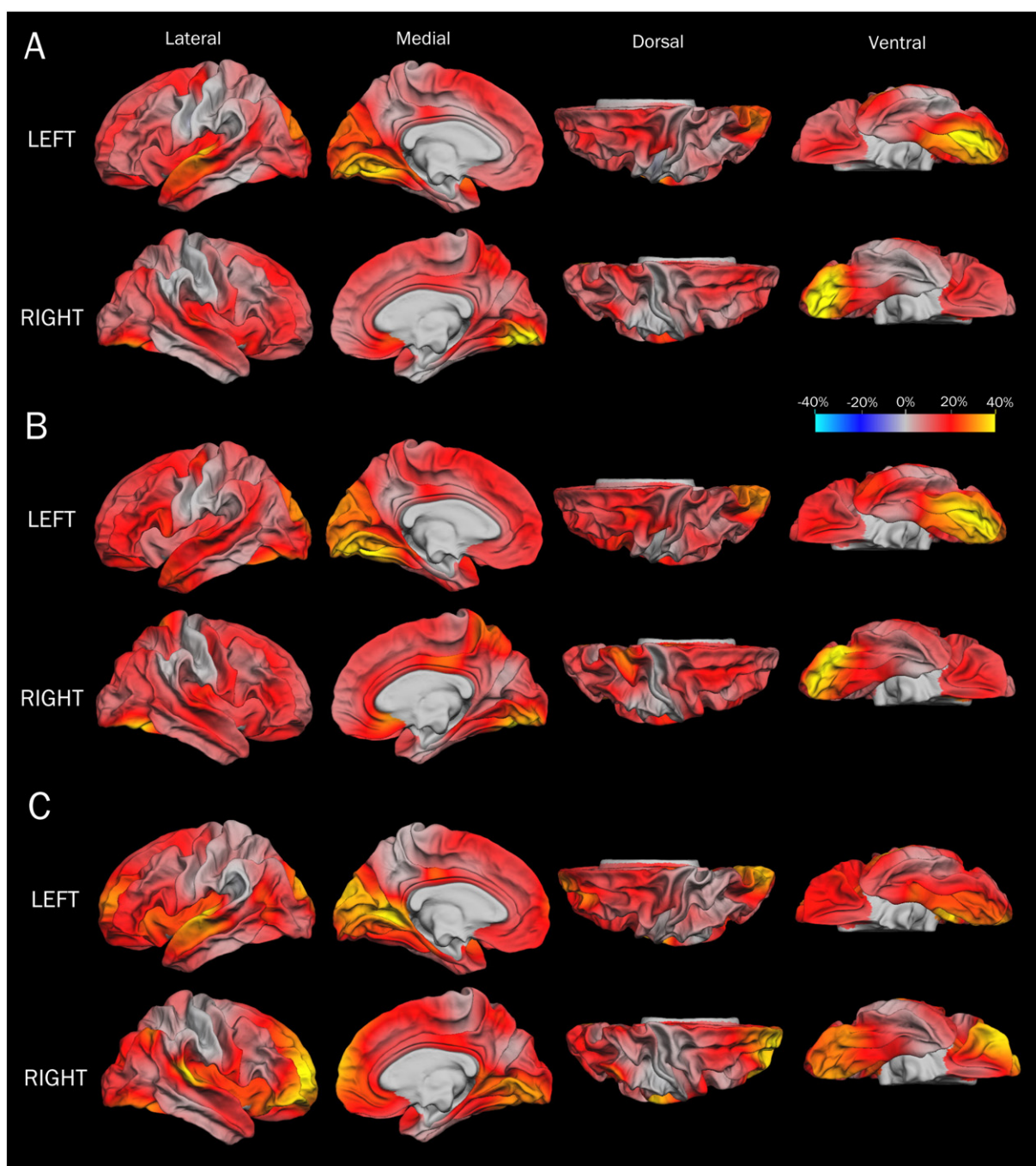
Fig. 1. Cortical surface area maps of explained variance in VLBW group. Maps of explained variance (r^2) for the association between test scores on the three VMI tests (A: copying, B: motor, C: visual) and cortical surface area in the VLBW sample. The r^2 is based on a GLM with cortical surface area as dependent variable, sex as categorical predictor, and age at MRI scan and one of the VMI test scores as continuous predictor. $r^2 = (F / (F + df))$. Abbreviations: FDR, false discovery rate; GLM, general linear model; VLBW, very low birth weight; VMI, Beery–Buktenica Developmental Test of Visual–Motor Integration—V.

variance values were as low as 10% in the least correlated regions that survived significance testing. There were no significant findings in the control group.

Cortical thickness

In the VLBW group, the general linear model identified regions with a significant relationship between cortical thickness and visual test scores but not the other two VMI tests (Fig. 3). The findings were mainly in the lateral occipito-temporo-parietal junction, the superior temporal gyrus and insula (extending into inferior frontal gyrus), as well as

superior parietal regions including superior parietal gyrus and postcentral gyrus. There were fewer findings on the medial side, in particular some in the left precuneus, cuneus, and medial occipital gyrus. There were no significant findings in the control group.

Group differences

There were significant differences in cortical surface area between the VLBW group and the control group. The VLBW group showed reduced cortical surface area primarily in frontal, temporal, and parietal lobes. Cortical thinning was observed in the left parietal and temporal
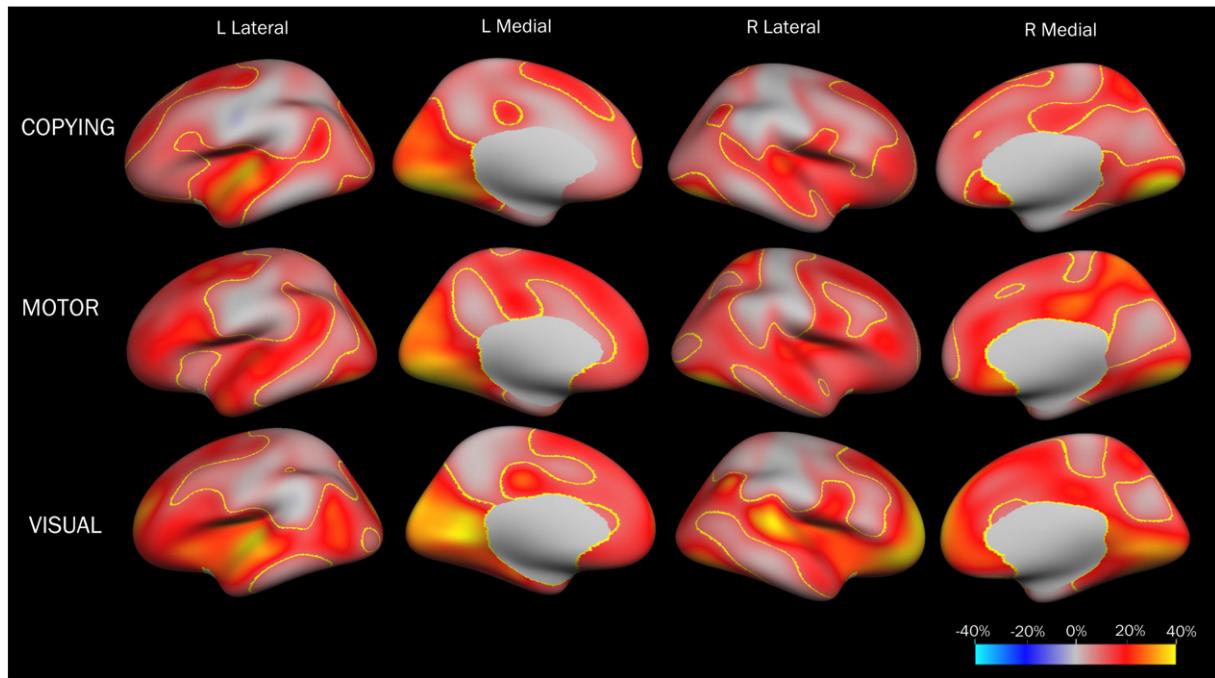
Fig. 2. Labeled cortical surface area maps of explained variance in VLBW group. Maps of explained variance (r^2) for the association between test scores on the three VMI tests and cortical surface area in the VLBW sample, with suprathreshold regions outlined in yellow. Suprathreshold regions are cortical regions that survived the significance test and a subsequent 5% FDR correction. The significance tests and the effect size estimates (r^2) are based on fitting GLMs with cortical surface area as dependent variable, sex as categorical predictor, and age at MRI scan and one of the VMI test scores as continuous predictor. Contrast vectors were set to test for a relationship between performance on each of the VMI tests (copying, motor, visual) and cortical surface area. The p-maps were thresholded and multiple comparisons were corrected for with a 5% FDR that was applied co-jointly across the hemispheres. To create a map illustrating both effect sizes as well as which regions contain statistically significant findings, a label was created in FreeSurfer containing vertices that survived the significance test (including FDR). This label was subsequently overlaid on the effect size map. Abbreviations: FDR, false discovery rate; GLM, general linear model; VLBW, very low birth weight; VMI, Beery–Buktenica Developmental Test of Visual–Motor Integration—V.

lobes and cortical thickening in frontal regions bilaterally; however there was no significant difference in mean global cortical thickness between groups. These group differences have previously been reported by our group (Skranes et al., 2013; Bjuland et al., 2013) and are therefore not presented here.

DTI findings

Fractional anisotropy in VLBW group

In the VLBW group, all three visual–motor test scores correlated positively with FA ($p < 0.05$; red voxels in Fig. 4). DTI analysis demonstrated
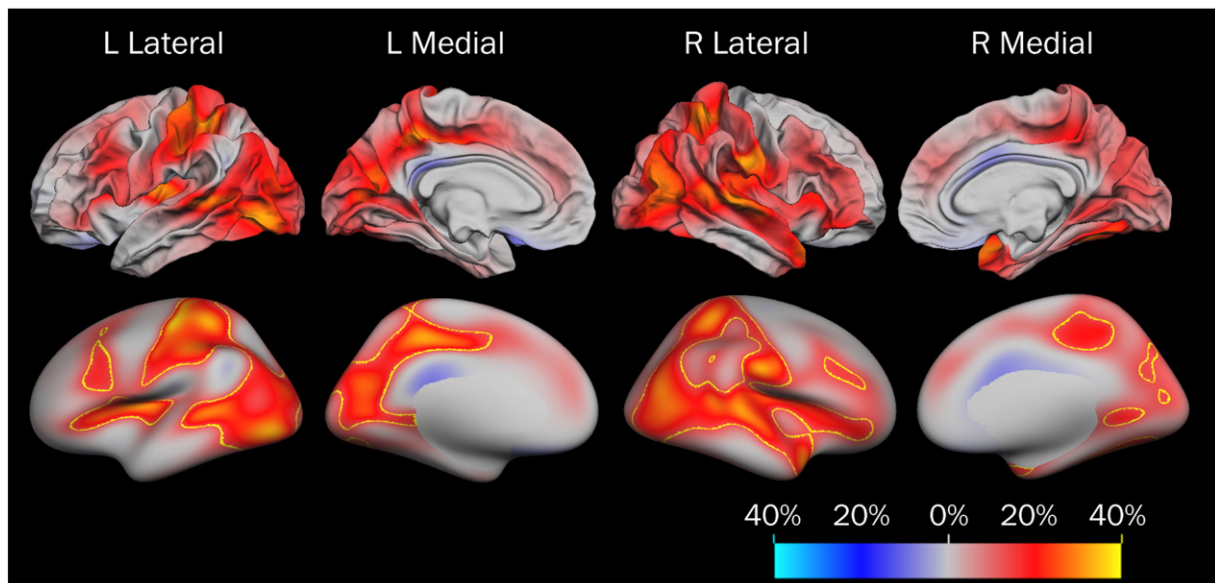

Fig. 3. Cortical thickness maps of explained variance in the VLBW group for VMI visual test scores, shown without and with suprathreshold labeling. Maps of explained variance (r^2) for the association between test scores on the VMI visual test and cortical thickness in the VLBW sample (top row), with suprathreshold regions outlined in yellow (bottom row). The maps were produced from GLMs with cortical thickness as dependent variable at each location (vertex) across the surface, and visual test scores as independent variable, covarying for age and sex. To create a map illustrating both effect sizes as well as which regions contain statistically significant findings, a label was created in FreeSurfer containing vertices that survived the significance test (including FDR). This label was subsequently overlaid on the effect size map, as shown in the bottom row. Abbreviations: FDR, false discovery rate; GLM, general linear model; VLBW, very low birth weight; VMI, Beery–Buktenica Developmental Test of Visual–Motor Integration—V.
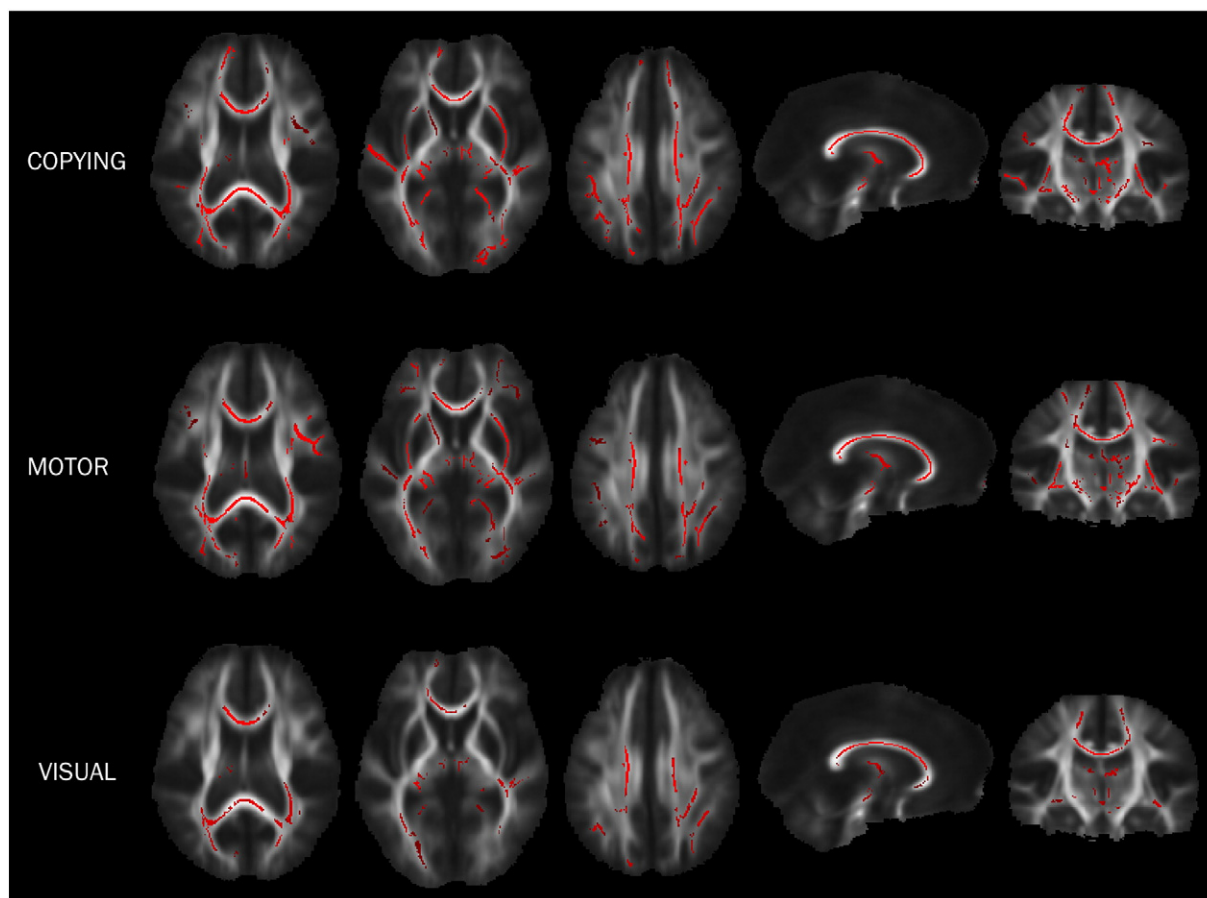
Fig. 4. Fractional anisotropy and visual–motor score correlations in the VLBW group. White matter areas demonstrating a positive correlation (voxels in red) between VMI test scores and fractional anisotropy in the VLBW group, based on DTI analysis in TBSS and Randomise ($p < 0.05$, nonparametric permutation test, corrected for multiple comparisons, gender and age at MRI). Images are displayed in radiological convention (right brain on left side). Abbreviations: DTI, diffusion tensor imaging; TBSS, Tract-Based Spatial Statistics; VLBW, very low birth weight; VMI, Beery–Buktenica Developmental Test of Visual–Motor Integration—V.

significant positive correlations between FA and copying scores in the corpus callosum (extending rostrally in the right hemisphere), optic radiation, bilateral inferior longitudinal fasciculus, bilateral inferior fronto-occipital fasciculus (more strongly in the right hemisphere), bilateral uncinate fasciculus, bilateral external capsules, and to some extent bilaterally in the anterior thalamic radiation, as well as in the left superior longitudinal fasciculus and right internal capsule. For the motor test, reduced scores correlated with FA reductions in corpus callosum, bilateral inferior longitudinal fasciculus (more strongly in the right hemisphere), bilateral inferior fronto-occipital fasciculus (more strongly in the right hemisphere), bilateral uncinate fasciculus, and bilateral external capsules, as well as left superior longitudinal fasiculus, right internal capsule, and somewhat in the right anterior thalamic radiation and to lesser extent in the left anterior thalamic radiation. For the visual perception test, correlation between FA and score was less widespread compared to the other two tests and were mainly found in the corpus callosum, particularly in the body, and bilaterally in the posterior inferior fronto-occipital fasciculus and the anterior thalamic radiation.

Mean diffusivity and eigenvalue analysis in the VLBW group

In the VLBW group, MD was negatively correlated to all visual–motor test scores in white matter structures similar to but less widespread than the FA findings. Separating the three eigenvalues, the radial diffusivities λ_2 and λ_3 reflecting radial diffusivity showed negative correlations to scores in all three visual–motor test scores. The axial diffusivity λ_1 indicated a negative correlation in very few white matter

structures in relation to copying scores, but none with the motor or visual tests.

Findings in control group

FA, MD, and λ_1, λ_2, and λ_3 eigenvalues did not demonstrate significant correlations with any of the visual–motor test scores in the control group (data not shown). In a previous report on a subset of the same study population, Eikenes et al. (2011) showed group differences between preterm-born VLBW young adults and controls, examining relationships between DTI parameters, cognitive performance, and perinatal clinical data.

Discussion

In our VLBW young adult group, poorer visual–motor integration performance was related to thinner cortex in several regions, reduced cortical surface area in all four cerebral lobes, including regions important for visual association and motor function, and reduced FA in several association tracts. We have thus identified gray and white matter structures that appear to be sensitive to perinatal injury and visual–motor integration. These structural alterations related to perceptual and motor coordination deficits persist even at entry to adulthood and underscore the importance of these gray and white matter structures for normal visual–motor functioning in the VLBW population.

VLBW individuals performed significantly worse on the VMI copying and motor tests than the control group, and their scores on all three VMI tests had significant relationships to surface area in widespread cortical regions, with the superior temporal gyrus, the insula, and the medial

occipital lobe in conjunction with the posterior ventral temporal lobe (lingual gyrus and fusiform gyrus to a lesser extent) being the most consistently significant regions across the three VMI tests. FA in the corpus callosum, bilateral inferior fronto-occipital fasciculus, and bilateral anterior thalamic radiation correlated positively to scores on all three VMI tests, and radial diffusivities λ_2 and λ_3 showed negative correlations to all three test scores in the VLBW group. There were no significant relationships between VMI test scores and cortical morphometry or DTI in the control group.

Cortical surface area and thickness

Morphometric analyses on cortical surface area and thickness identified several cortical regions that showed significant relationships to visual–motor performance. The regions that showed the highest explained variance were similar across all three tests, including the superior temporal gyrus, insula, and medial occipital lobe in conjunction with the posterior ventral temporal lobe (Fig. 1). In VLBW individuals, it appears that these regions may experience injury related to preterm birth. Consistent with this, Nosarti et al. (2008) found that gestational age in very preterm adolescents was linearly associated with decreased gray matter bilaterally in portions of the superior temporal gyri and the insula, which has been linked to various cognitive functions, speech, and articulatory control processes (Ackermann and Riecker, 2010).

Cortical thickness in the VLBW group exhibited a significant relationship to visual scores, and several of the implicated cortical regions are believed to be involved in visual and motor function. Lesion studies have identified a possible role of superior parietal regions in visually guided movements and reaching (Vesia and Crawford, 2012), while the precuneus has diverse and as yet poorly demarcated functions ranging from visual–spatial imagery and mental representations of the self (Cavanna and Trimble, 2006) to proprioceptive input from the arm during tasks (Vesia and Crawford, 2012). The three VMI tests, which demand visual–spatial planning and fine motor execution, may therefore be expected to draw upon the functions of these cortical regions.

DTI findings

Lower FA was found to correlate to lower VMI scores in the VLBW group. However, when looking at the eigenvalues, only radial diffusivities were found to correlate negatively with VMI scores, while axial diffusivity was only found to correlate with the copying test in a few structures. This is in line with previous results, in which we demonstrated that the reduced FA in the same VLBW study group was driven primarily by an increase in radial diffusivity (Eikenes et al., 2011).

The corpus callosum was implicated in our analyses for each of the three VMI tests. This major white matter structure is widely reported to be impacted by preterm birth, and studies have demonstrated lower FA in the corpus callosum compared to controls at term-equivalent age (Lepomäki et al., 2012) and during adolescence and young adulthood (Nagy et al., 2009; Eikenes et al., 2011). Groeschel et al. (2014) found higher axial diffusivity in preterm-born adolescents in the corpus callosum body for fibers connecting premotor areas, while Thompson et al. (2012) found higher diffusivity in the splenium at term-equivalent age associated with impaired motor development at two years. Smaller corpus callosum size, especially posteriorly, has been associated with lower VMI copying scores (Rademaker et al., 2004). We have previously reported significant positive correlation between visual acuity and FA in the splenium and midbody of the corpus callosum in the VLBW group (Lindqvist et al., 2011).

In the optic radiation, we found a positive correlation between FA and the copying scores in the VLBW group, which expands upon our previous findings of significantly reduced FA and increased MD in optic radiation in VLBW young adults compared to controls (Eikenes et al., 2011). DTI assessments of premature infants have indicated a significant positive correlation between optic radiation fractional anisotropy and visual function (Berman et al., 2009; Bassi et al., 2008). Thompson et al. (2013) also found higher diffusivity in the optic radiation of very preterm-born children at age seven compared to controls and suggested that optic radiation diffusion values may have a structure–function relationship with visual functions that rely on visual cortex processing.

FA in several major white matter structures, including long-range association tracts, correlated positively to VMI test scores. FA bilaterally in the uncinate fasciculus, a long-range white matter association tract that connects the orbitofrontal cortex to the anterior temporal lobes, correlated positively to scores on the copying and motor tests in the VLBW group. Moreover, FA in the inferior longitudinal fasciculus also correlated positively to copying and motor scores. Ortibus et al. (2012) found lower FA in the inferior longitudinal fasciculus in children with visual perceptual impairment compared to typically developing children and argued that this tract plays a role in object recognition. However, linkages between cognitive function and white matter findings in the inferior longitudinal fasciculus should be interpreted with caution, as it is believed to be involved in wide-ranging capacities including thought disorders, visual emotion, cognitive impairments, and language (Ashtari, 2012; Mandonnet et al., 2007). In addition, we identified positive correlations between copying and motor scores with FA in the external capsule and left superior longitudinal fasciculus, which along with the uncinate fasciculus have been shown to have lower FA in preterm-born individuals compared with controls (Duerden et al., 2013; Eikenes et al., 2011; Skranes et al., 2007). Integrity in these white matter structures may therefore be particularly sensitive to persistent white matter disturbances related to preterm birth.

It is difficult to translate DTI measures into specific physiological features (Pandit et al., 2013). However, it is possible that the reduced FA in these regions in the VLBW group is caused by decreased or aberrant myelination, as evidenced by increased radial diffusion (Cheong et al., 2009; Song et al., 2005). Nonetheless, white matter imaging may be able to detect structural alterations in motor pathways even where standard MRI does not indicate brain injury in preterm-born infants (Anjari et al., 2007; Hüppi and Dubois, 2006) and adolescents (Groeschel et al., 2014) and is therefore an important clinical neuroimaging tool for the preterm-born population.

Potential relationships between gray and white matter findings in the VLBW group

This study raises several important questions about the relationship between gray and white matter development in VLBW individuals through adolescence and into adulthood. Several white matter structures implicated in our DTI analysis connect to cortical regions in which VMI test scores were significantly related to surface area and cortical thickness, including in regions implicated in visual association and motor processing. Thus, by connecting gray and white matter analyses to cognitive data, we have identified putative gray–white matter networks in which structural integrity appears to relate to visual–motor performance in the VLBW population.

Copying and motor scores in the VLBW group correlated to FA in the inferior longitudinal fasciculus, an association pathway whose fibers connect the occipital and anterior temporal lobe and originates from the cuneus, lateral occipital gyrus, and posterior lingual and fusiform gyri (Catani et al., 2003), cortical regions which showed a high proportion of surface area significantly related to VMI test scores (Table 1). Long inferior longitudinal fasciculus fibers connect visual association with parahippocampal areas, while its short fibers connect regions related to primary visual processing and visual association including the inferior parietal lobe (Aralasmak et al., 2006). Both of these cortical targets also showed strong relationships between surface area and test scores in the VLBW cohort.

Scores on all three VMI tests correlated positively to FA in the inferior fronto-occipital fasciculus, a white matter tract important for connecting visual association areas with primary motor frontal eye fields, as well as for relaying elementary visual information (Aralasmak et al., 2006). The inferior fronto-occipital fasciculus connects the posterior temporal, orbito-frontal, and occipital regions (Ashtari et al., 2012), and we found large proportions of surface area in occipital regions, especially in the left hemisphere, significantly related to scores on all three visual–motor tests.

Finally, we identified significant DTI correlations in several other major association tracts and white matter structures which have cortical targets important for visual and motor function. The uncinate fasciculus, a major long association tract with FA significantly related to scores on the copying and motor tests in our study, links the frontal and temporal lobes including regions involved in multimodal association and event-related memory (Catani et al., 2002). The superior longitudinal fasciculus, where FA in the left hemisphere positively correlated with copying and motor scores, is another major association bundle connecting the external surface of the temporoparieto-occipital regions with the frontal lobe and is thought to be related to visuospatial processing and spatial attention (Thiebaut de Schotten et al., 2011). The internal capsule contains corticofugal motor and thalamocortical sensory projection fibers (Aralasmak et al., 2006) and was in the right hemisphere also positively correlated with copying and motor scores.

We speculate that the structural deviations seen in the VLBW group may be due to perinatal injury and cause reduced scores on these visual–motor tests. It is also possible that the widespread findings for cortical surface area reflect a more general relationship between cognition and aberrant brain development in the VLBW group. These relationships may be stronger in some regions with regard to perceptual functioning but may suggest larger-scale relationships across the cortex.

Cognitive findings and clinical implications

The VLBW group performed significantly worse on the copying and motor tests than term-born individuals, as expected. This finding is consistent with earlier literature concerning preterm birth, although most studies have evaluated school-aged children in contrast to our young adults (Geldof et al., 2012; Davis et al., 2005; Hard et al., 2000; Goyen et al., 1998; Molloy et al., 2014). Preterm-born individuals have demonstrated worse performance on simple visual–motor tasks and are thought to have a different, rather than merely delayed, developmental trajectory for visual–motor processes compared to controls (Van Braeckel et al., 2010; Narberhaus et al., 2009; Sullivan and Margaret, 2003; Martinussen et al., 2009).

Visual–motor impairment can have far-reaching consequences, including in the classroom, where motor coordination and fine motor skills are fundamental for everyday tasks. Preterm-born school-aged children have demonstrated worse handwriting performance, including significantly lower legibility and slower speed (Feder et al., 2005). Recent studies have begun to highlight the role of white matter (Saygin et al., 2013; Aeby et al., 2013) and cortical thickness (Clark et al., 2014) structural alterations as biomarkers of latent developmental problems, such as dyslexia. Our results indicate that diminished motor coordination in the VLBW cohort evident at earlier ages persists even through early adulthood.

By contrast, scores on the visual matching subtest were nearly the same between the groups. In a recent functional MRI study on visual–perceptual function, Narberhaus et al. (2009) found that very preterm-born adolescents did not demonstrate performance deficits on a visual–perceptual learning task inside the MRI scanner yet showed different patterns of brain activation compared to controls. It may therefore be possible that preterm VLBW individuals develop compensatory connections to improve visual processing, especially in the absence of a stronger demand on motor function.

Visual–motor integration, motor coordination, and visual–perceptual impairments may have a common etiology in preterm VLBW individuals. Perinatal brain injury that affects posterior deep white matter connectivity may have consequences for both visual and perceptual cortical regions (Skranes et al., 2007). Preterm-born individuals are at risk for periventricular leukomalacia (Volpe, 2001), and subsequent damage to the developing sensory, motor, and cognitive pathways may result in modified target regions or tract directions which are different from what is observed in term-born individuals (Tzarouchi et al., 2011).

Important developmental events unfold during 24 to 40 weeks of gestation and may enhance the fetus's vulnerability to ischemia, inflammation, excitotoxicity, and free-radical attack, and possibly other exogenous insults like drugs and undernutrition (Volpe, 2009; Dobbing, 1974). Groppo et al. (2014) posit that the developing visual system undergoes significant maturation and vulnerability between 32 weeks of gestation and term–equivalent age. Events during this timeframe may also contribute to visual–motor integration abilities.

Strengths and limitations

A strength of this study is the long-term follow-up of the two study groups, which were recruited at birth and equivalent in terms of maternal age at childbirth and socioeconomic status. The groups have been followed prospectively with comprehensive multidisciplinary clinical, cognitive, and MRI assessments at different ages. Through a drop-out analysis, we found no differences in background characteristics between those who participated and those who chose not to participate in the early adolescence and early adulthood follow-up sessions, which reduces the likelihood that the results were influenced by selection bias. In order to reduce the risk of information bias, the cognitive testing was performed by two trained examiners blinded to group adherence and former medical history.

About 56% of those eligible from the cohort participated at the early adulthood follow-up with a full perceptual assessment and MRI. While this percentage is lower than ideal, it is comparable to other long-term follow-up studies assessing adolescents and young adults, where high drop-out rates are common (Hille et al., 2005). Cases lost to follow-up are often selective, and mothers with low educational attainment and those with children with serious developmental delays or disabilities are most likely to drop out (Wolke et al., 1995). If that is the case in our study, this would most likely have led to an underestimation rather than an overestimation of the prevalence of problems reported.

Furthermore, in the control group, we did not find significant relationships between gray and white matter structure and VMI scores, consistent with previous reports from our group. However, a few studies do report significant structure–function relationships in healthy controls (see e.g., Squeglia et al., 2013), so it is thinkable that such correlations may also exist in term-born children.

Finally, our relatively small number of participants means that we have limited power to detect minor group and sex differences and must therefore interpret non-significant results with caution. Because of the limited sample size, differences in VLBW subgroups based on cut-off values for birth weight, gestational age, and other perinatal variables, were not investigated. Additional details on the reasons behind the VLBW would have been interesting to assess; for instance, whether individuals who experienced fetal growth restriction exhibit differential perinatal injuries or developmental trajectories.

Conclusions

Our results indicate an increased risk of visual–motor integration deficits in early adulthood for individuals born preterm with VLBW. Alterations in white matter tracts containing primary and secondary visual and motor fibers and reduced surface area of visual–perceptual cortical regions, both of which correlated to reduced test scores, may indicate a structure–function relationship that entails both long-lasting

effects of early perinatal brain injury and persistent visual–motor perceptual deficits in VLBW individuals who have reached young adulthood.

Acknowledgments

Appendix A. Supplementary data

Supplementary data to this article can be found online at http://dx.doi.org/10.1016/j.neuroimage.2015.01.019.

References

Aarnoudse-Moens, C.S.H., Smidts, D.P., Oosterlaan, J., Duivenvoorden, H.J., Weisglas-Kuperus, N., 2009. Executive function in very preterm children at early school age. J. Abnorm. Child Psychol. 13 (7), 981–993.

Ackermann, H., Riecker, A., 2010. The contribution(s) of the insula to speech production: a review of the clinical and functional imaging literature. Brain Struct. Funct. 214 (5–6), 419–433 (Jun).

Aeby, A., De Tiège, X., Creuzil, M., David, P., Balériaux, D., Van Overmeire, B., Metens, T., Van Bogaert, P., 2013. Language development at 2 years is correlated to brain microstructure in the left superior temporal gyrus at term equivalent age: a diffusion tensor imaging study. NeuroImage 78, 145–151 (Sep).

Anjari, M., Srinivasan, L., Allsop, J.M., Hajnal, J.V., Rutherford, M.A., Edwards, A.D., Counsell, S.J., 2007. Diffusion tensor imaging with tract-based spatial statistics reveals local white matter abnormalities in preterm infants. NeuroImage 35 (3), 1021–1027 (Apr 15).

Aralasmak, A., Ulmer, J.L., Kocak, M., Salvan, C.V., Hillis, A.E., Yousem, D.M., 2006. Association, commissural, and projection pathways and their functional deficit reported in literature. J. Comput. Assist. Tomogr. 30 (5), 695–715 (Sep–Oct).

Ashtari, M., 2012. Anatomy and functional role of the inferior longitudinal fasciculus: a search that has just begun. Dev. Med. Child Neurol. 54 (1), 6–7 (Jan).

Aylward, G.P., 2005. Neurodevelopmental outcomes of infants born prematurely. J. Dev. Behav. Pediatr. 26, 427–440.

Basser, P.J., Pierpaoli, C., 1996. Microstructural and physiological features of tissues elucidated by quantitative-diffusion-tensor MRI. J. Magn. Reson. B. 111, 209–219.

Bassi, L., Ricci, D., Volzone, A., et al., 2008. Probabilistic diffusion tractography of the optic radiations and visual function in preterm infants at term equivalent age. Brain 131, 573–582.

Beery, K.E., Buktenica, N.A., Beery, N.A., 2004. The Beery–Buktenica Developmental Test of Visual–Motor Integration: Administration, Scoring and Teaching Manual. 5th edition. NCS Pearson, Minneapolis, MN.

Berman, J.I., Glass, H.C., Miller, S.P., Mukherjee, P., Ferriero, D.M., Barkovich, A.J., et al., 2009. Quantitative fiber tracking analysis of the optic radiation correlated with visual performance in premature newborns. Am. J. Neuroradiol. 30, 120–124.

Bjuland, K.J., Løhaugen, G.C., Martinussen, M., Skranes, J., 2013. Cortical thickness and cognition in very-low-birth-weight late teenagers. Early Hum. Dev. 89 (6), 371–380 (Jun).

Bjuland, K.J., Rimol, L.M., Løhaugen, G.C., Skranes, J., 2014. Brain volumes and cognitive function in very-low-birth-weight (VLBW) young adults. Eur. J. Paediatr. Neurol. 18 (5), 578–590 (Sep).

Bora, S., Pritchard, V.E., Chen, Z., Inder, T.E., Woodward, L.J., 2014. Neonatal cerebral morphometry and later risk of persistent inattention/hyperactivity in children born very preterm. J. Child Psychol. Psychiatry 55 (7), 828–838 (Jul).

Catani, M., Howard, R.J., Pajevic, S., Jones, D.K., 2002. Virtual in vivo interactive dissection of white matter fasciculi in the human brain. NeuroImage 17 (1), 77–94 (Sep).

Catani, M., Jones, D.K., Donato, R., ffytche, D.H., 2003. Occipito-temporal connections in the human brain. Brain 126 (Pt 9), 2093–2107 (Sep).

Cavanna, A.E., Trimble, M.R., 2006. The precuneus: a review of its functional anatomy and behavioural correlates. Brain 129 (Pt 3), 564–583 (Mar).

Chau, V., Taylor, M.J., Miller, S.P., 2013. Visual function in preterm infants: visualizing the brain to improve prognosis. Doc. Ophthalmol. 127 (1), 41–55 (Aug).

Cheong, J.L., Thompson, D.K., Wang, H.X., Hunt, R.W., Anderson, P.J., Inder, T.E., Doyle, L.W., 2009. Abnormal white matter signal on MR imaging is related to abnormal tissue microstructure. AJNR Am. J. Neuroradiol. 30 (3), 623–628 (Mar).

Clark, K.A., Helland, T., Specht, K., Narr, K.L., Manis, F.R., Toga, A.W., Hugdahl, K., 2014. Neuroanatomical precursors of dyslexia identified from pre-reading through to age 11. Brain 137 (12), 3136–3144 (Dec).

Constable, R.T., Ment, L.R., Vohr, B.R., Kesler, S.R., Fulbright, R.K., Lacadie, C., Delancy, S., Katz, K.H., Schneider, K.C., Schafer, R.J., Makuch, R.W., Reiss, A.R., 2008. Prematurely born children demonstrate white matter microstructural differences at 12 years of

age, relative to term control subjects: an investigation of group and gender effects. Pediatrics 121 (2), 306–316 (Feb).

Dale, A.M., Sereno, M.I., 1993. Improved localization of cortical activity by combining EEG and MEG with MRI cortical surface reconstruction: a linear approach. J. Cogn. Neurosci. 5 (2), 162–176 (Spring).

Dale, A.M., Fischl, B., Sereno, M.I., 1999. Cortical surface-based analysis. I. Segmentation and surface reconstruction. NeuroImage 9 (2), 179–194 (Feb).

Davis, D.W., Burns, B.M., Wilkerson, S.A., Steichen, J.J., 2005. Visual perceptual skills in children born with very low birth weights. J. Pediatr. Health Care 19, 363–368.

de Kieviet, J.F., Zoetebier, L., van Elburg, R.M., Vermeulen, R.J., Oosterlaan, J., 2012. Brain development of very preterm and very low-birthweight children in childhood and adolescence: a meta-analysis. Dev. Med. Child Neurol. 54 (4), 313–323 (Apr).

Desikan, R.S., Ségonne, F., Fischl, B., Quinn, B.T., Dickerson, B.C., Blacker, D., Buckner, R.L., Dale, A.M., Maguire, R.P., Hyman, B.T., Albert, M.S., Killiany, R.J., 2006. An automated labeling system for subdividing the human cerebral cortex on MRI scans into gyral based regions of interest. NeuroImage 31 (3), 968–980 (Jul 1).

Dobbing, J., 1974. The later growth of the brain and its vulnerability. Pediatrics 53 (1), 2–6 (Jan).

Dubois, J., Dehaene-Lambertz, G., Kulikova, S., Poupon, C., Hüppi, P.S., Hertz-Pannier, L., 2014. The early development of brain white matter: a review of imaging studies in fetuses, newborns and infants. Neuroscience 276, 48–71 (Sep 12).

Duerden, E.G., Card, D., Lax, I.D., Donner, E.J., Taylor, M.J., 2013. Alterations in frontostriatal pathways in children born very preterm. Dev. Med. Child Neurol. 55 (10), 952–958 (Oct).

Eikenes, L., Løhaugen, G.C., Brubakk, A.M., Skranes, J., Håberg, A.K., 2011. Young adults born preterm with very low birth weight demonstrate widespread white matter alterations on brain DTI. NeuroImage 54 (3), 1774–1785 (Feb 1).

Evensen, K.A., Vik, T., Helbostad, J., et al., 2004. Motor skills in adolescents with low birth weight. Arch. Dis. Child Fetal Neonatal Ed. 89, F451–F455.

Evensen, K.A., Lindqvist, S., Indredavik, M.S., et al., 2009. Do visual impairments affect risk of motor problems in preterm and term low birth weight adolescents? Eur. J. Paediatr. Neurol. 13, 47–56.

Feder, K.P., Majnemer, A., Bourbonnais, D., Platt, R., Blayney, M., Synnes, A., 2005. Handwriting performance in preterm children compared with term peers at age 6 to 7 years. Dev. Med. Child Neurol. 47 (3), 163–170 (Mar).

Fischl, B., Dale, A.M., 2000. Measuring the thickness of the human cerebral cortex from magnetic resonance images. Proc. Natl. Acad. Sci. U. S. A. 97 (20), 11050–11055 (Sep 26).

Fischl, B., Sereno, M.I., Dale, A.M., 1999a. Cortical surface-based analysis. II: inflation, flattening, and a surface-based coordinate system. NeuroImage 9 (2), 195–207 (Feb).

Fischl, B., Sereno, M.I., Tootell, R.B., Dale, A.M., 1999b. High-resolution intersubject averaging and a coordinate system for the cortical surface. Hum. Brain Mapp. 8 (4), 272–284.

Fischl, B., Liu, A., Dale, A.M., 2001. Automated manifold surgery: constructing geometrically accurate and topologically correct models of the human cerebral cortex. IEEE Trans. Med. Imaging 20 (1), 70–80 (Jan).

Fischl, B., Salat, D.H., Busa, E., Albert, M., Dieterich, M., Haselgrove, C., van der Kouwe, A., Killiany, R., Kennedy, D., Klaveness, S., Montillo, A., Makris, N., Rosen, B., Dale, A.M., 2002. Whole brain segmentation: automated labeling of neuroanatomical structures in the human brain. Neuron 33 (3), 341–355 (Jan 31).

Fischl, B., Salat, D.H., van der Kouwe, A.J., Makris, N., Ségonne, F., Quinn, B.T., Dale, A.M., 2004a. Sequence-independent segmentation of magnetic resonance images. NeuroImage 23 (Suppl. 1), S69–S84.

Fischl, B., van der Kouwe, A., Destrieux, C., Halgren, E., Ségonne, F., Salat, D.H., Busa, E., Seidman, L.J., Goldstein, J., Kennedy, D., Caviness, V., Makris, N., Rosen, B., Dale, A.M., 2004b. Automatically parcellating the human cerebral cortex. Cereb. Cortex 14 (1), 11–22 (Jan).

Geldof, C.J., van Wassenaer, A.G., de Kieviet, J.F., Kok, J.H., Oosterlaan, J., 2012. Visual perception and visual–motor integration in very preterm and/or very low birth weight children: a meta-analysis. Res. Dev. Disabil. 33 (2), 726–736 (Mar–Apr).

Giménez, M., Junqué, C., Narberhaus, A., Caldú, X., Salgado-Pineda, P., Bargalló, N., Segarra, D., Botet, F., 2004. Hippocampal gray matter reduction associates with memory deficits in adolescents with history of prematurity. NeuroImage 23 (3), 869–877 (Nov).

Goyen, T.A., Lui, K., Woods, R., 1998. Visual–motor, visual–perceptual, and fine motor outcomes in very-low-birthweight children at 5 years. Dev. Med. Child Neurol. 40, 76–81.

Groeschel, S., Tournier, J.D., Northam, G.B., Baldeweg, T., Wyatt, J., Vollmer, B., Connelly, A., 2014. Identification and interpretation of microstructural abnormalities in motor pathways in adolescents born preterm. NeuroImage 87, 209–219 (Feb 15).

Groppo, M., Ricci, D., Bassi, L., Merchant, N., Doria, V., Arichi, T., Allsop, J.M., Ramenghi, L., Fox, M.J., Cowan, F.M., Counsell, S.J., Edwards, A.D., 2014. Development of the optic radiations and visual function after premature birth. Cortex 56, 30–37 (Jul).

Han, X., Jovicich, J., Salat, D., van der Kouwe, A., Quinn, B., Czanner, S., Busa, E., Pacheco, J., Albert, M., Killiany, R., Maguire, P., Rosas, D., Makris, N., Dale, A., Dickerson, B., Fischl, B., 2006. Reliability of MRI-derived measurements of human cerebral cortical thickness: the effects of field strength, scanner upgrade and manufacturer. Neuroimage 32, 180–194.

Hard, A.L., Niklasson, A., Svensson, E., Hellstrom, A., 2000. Visual function in school-aged children born before 29 weeks of gestation: a population-based study. Dev. Med. Child Neurol. 42, 100–105.

Healy, E., Reichenberg, A., Nam, K.W., Allin, M.P., Walshe, M., Rifkin, L., Murray, S.R., Nosarti, C., 2013. Preterm birth and adolescent social functioning-alterations in emotion-processing brain areas. J. Pediatr. 163 (6), 1596–1604 (Dec).

Hellgren, K., Hellstrom, A., Jacobson, L., et al., 2007. Visual and cerebral sequelae of very low birth weight in adolescents. Arch. Dis. Child Fetal Neonatal Ed. 92, F259–F264.

Hille, E.T., den Ouden, A.L., Stuifbergen, M.C., Verrips, G.H., Vogels, A.G., Brand, R., Gravenhorst, J.B., Verloove-Vanhorick, S.P., 2005. Is attrition bias a problem in neonatal follow-up? Early Hum. Dev. 81 (11), 901–908 (Nov).

Hollingshead AB. Two factor index of social position. Mimeo. New Haven, Connecticut: Yale University. 1957.

Hua, K., Zhang, J., Wakana, S., Jiang, H., Li, X., Reich, D.S., Calabresi, P.A., Pekar, J.J., van Zijl, P.C., Mori, S., 2008. Tract probability maps in stereotaxic spaces: analyses of white matter anatomy and tract-specific quantification. NeuroImage 39 (1), 336–347 (Jan 1).

Hüppi, P.S., Dubois, J., 2006. Diffusion tensor imaging of brain development. Semin. Fetal Neonatal Med. 11 (6), 489–497 (Dec).

Iwata, S., Nakamura, T., Hizume, E., Kihara, H., Takashima, S., Matsuishi, T., Iwata, O., 2012. Qualitative brain MRI at term and cognitive outcomes at 9 years after very preterm birth. Pediatrics 129 (5), e1138–e1147 (May).

Johansen-Berg, H., Behrens, T.E.J. (Eds.), 2009. Diffusion MRI: From Quantitative Measurement to In-vivo Neuroanatomy. Academic Press, London.

Jovicich, J., Czanner, S., Greve, D., Haley, E., van der Kouwe, A., Gollub, R., Kennedy, D., Schmitt, F., Brown, G., Macfall, J., Fischl, B., Dale, A., 2006. Reliability in multi-site structural MRI studies: effects of gradient non-linearity correction on phantom and human data. NeuroImage 30 (2), 436–443 (Apr 1).

Kim, D.J., Davis, E.P., Sandman, C.A., Sporns, O., O'Donnell, B.F., Buss, C., Hetrick, W.P., 2014. Longer gestation is associated with more efficient brain networks in preadolescent children. NeuroImage 100, 619–627 (Oct 15).

Krageloh-Mann, I., Toft, P., Lunding, J., et al., 1999. Brain lesions in preterms: origin, consequences and compensation. Acta Paediatr. 88, 897–908.

Lax, I.D., Duerden, E.G., Lin, S.Y., Mallar Chakravarty, M., Donner, E.J., Lerch, J.P., Taylor, M.J., 2013. Neuroanatomical consequences of very preterm birth in middle childhood. Brain Struct. Funct. 218 (2), 575–585 (Mar).

Le Bihan, D., Johansen-Berg, H., 2012. Diffusion MRI at 25: exploring brain tissue structure and function. NeuroImage 61 (2), 324–341 (Jun).

Lepomäki, V., Paavilainen, T., Matomäki, J., Hurme, S., Haataja, L., Lapinleimu, H., Liisa Lehtonen, L., Komu, M., Parkkola, R., PIPARI Study Group, 2012. Effect of antenatal growth and prematurity on brain white matter: diffusion tensor study. Pediatr. Radiol. 42 (6), 692–698 (Jun).

Lindqvist, S., Vik, T., Indredavik, M.S., Brubakk, A.M., 2007. Visual acuity, contrast sensitivity, peripheral vision and refraction in low birthweight teenagers. Acta Ophthalmol. Scand. 85, 157–164.

Lindqvist, S., Vik, T., Indredavik, M.S., Skranes, J., Brubakk, A.M., 2008. Eye movements and binocular function in low birthweight teenagers. Acta Ophthalmol. 86, 265–274.

Lindqvist, S., Skranes, J., Eikenes, L., Haraldseth, O., Vik, T., Brubakk, A.M., Vangberg, T.R., 2011. Visual function and white matter microstructure in very-low-birth-weight (VLBW) adolescents—a DTI study. Vision Res. 51 (18), 2063–2070 (Sep 15).

Mandonnet, E., Nouet, A., Gatignol, P., Capelle, L., Duffau, H., 2007. Does the left inferior longitudinal fasciculus play a role in language? A brain stimulation study. Brain 130 (Pt 3), 623–629 (Mar).

Martinussen, M., Flanders, D.W., Fischl, B., et al., 2009. Segmental brain volumes and cognitive and perceptual correlates in 15-year-old adolescents with low birth weight. J. Pediatr. 155, 848–853.

McGrath, M., Sullivan, M., 2002. Birth weight, neonatal morbidities, and school age outcomes in full-term and preterm infants. Issues Compr. Pediatr. Nurs. 25 (4), 231–254 (Oct–Dec).

Ment, L.R., Hirtz, D., Hüppi, P.S., 2009. Imaging biomarkers of outcome in the developing preterm brain. Lancet Neurol. 8 (11), 1042–1055 (Nov).

Mento, G., Bisiacchi, P.S., 2012. Neurocognitive development in preterm infants: insights from different approaches. Neurosci. Biobehav. Rev. 36 (1), 536–555 (Jan).

Molloy, C.S., Wilson-Ching, M., Doyle, L.W., Anderson, V.A., Anderson, P.J., Victorian Infant Collaborative Study Group, 2014. Visual memory and learning in extremely low-birth-weight/extremely preterm adolescents compared with controls: a geographic study. J. Pediatr. Psychol. 39 (3), 316–331 (Apr).

Mori, S., Wakana, S., Nagae-Poetscher, L.M., van Zijl, C.M., 2005. MRI Atlas of Human White Matter. Elsevier, Amsterdam.

Mullen, K.M., Vohr, B.R., Katz, K.H., Schneider, K.C., Lacadie, C., Hampson, M., Makuch, R.W., Reiss, A.L., Constable, R.T., Ment, L.R., 2011. Preterm birth results in alterations in neural connectivity at age 16 years. NeuroImage 54 (4), 2563–2570 (Feb 14).

Nagy, Z., Ashburner, J., Andersson, J., Jbabdi, S., Draganski, B., Skare, S., Böhm, B., Smedler, A.C., Forssberg, H., Lagercrantz, H., 2009. Structural correlates of preterm birth in the adolescent brain. Pediatrics 124 (5), e964–e972 (Nov).

Narberhaus, A., Lawrence, E., Allin, M.P., Walshe, M., McGuire, P., Rifkin, L., Murray, R., Nosarti, C., 2009. Neural substrates of visual paired associates in young adults with a history of very preterm birth: alterations in fronto-parieto-occipital networks and caudate nucleus. NeuroImage 47 (4), 1884–1893 (Oct 1).

Nichols, T.E., Holmes, A.P., 2002. Nonparametric permutation tests for functional neuroimaging: a primer with examples. Hum. Brain Mapp. 15 (1), 1–25 (Jan).

Nosarti, C., Rushe, T.M., Woodruff, P.W., Stewart, A.L., Rifkin, L., Murray, R.M., 2004. Corpus callosum size and very preterm birth: relationship to neuropsychological outcome. Brain 127 (Pt 9), 2080–2089 (Sep).

Nosarti, C., Giouroukou, E., Healy, E., Rifkin, L., Walshe, M., Reichenberg, A., Chitnis, X., Williams, S.C., Murray, R.M., 2008. Grey and white matter distribution in very preterm adolescents mediates neurodevelopmental outcome. Brain 131 (Pt 1), 205–217 (Jan).

Nosarti, C., Mechelli, A., Herrera, A., Walshe, M., Shergill, S.S., Murray, R.M., Rifkin, L., Allin, M.P., 2011. Structural covariance in the cortex of very preterm adolescents: a voxel-based morphometry study. Hum. Brain Mapp. 32 (10), 1615–1625 (Oct).

Oishi, K., Faria, A., van Zijl, C.M., Mori, S., 2011. MRI Atlas of Human White Matter. 2nd edition. Elsevier, Amsterdam.

Ortibus, E., Verhoeven, J., Sunaert, S., Casteels, I., de Cock, P., Lagae, L., 2012. Integrity of the inferior longitudinal fasciculus and impaired object recognition in children: a diffusion tensor imaging study. Dev. Med. Child Neurol. 54 (1), 38–43 (Jan).

Pandit, A.S., Ball, G., Edwards, A.D., Counsell, S.J., 2013. Diffusion magnetic resonance imaging in preterm brain injury. Neuroradiology 55 (Suppl. 2), 65–95 (Sep).

Panizzon, M.S., Fennema-Notestine, C., Eyler, L.T., Jernigan, T.L., Prom-Wormley, E., Neale, M., Jacobson, K., Lyons, M.J., Grant, M.D., Franz, C.E., Xian, H., Tsuang, M., Fischl, B., Seidman, L., Dale, A., Kremen, W.S., 2009. Distinct genetic influences on cortical surface area and cortical thickness. Cereb. Cortex 19 (11), 2728–2735 (Nov).

Platt, M.J., Cans, C., Johnson, A., et al., 2007. Trends in cerebral palsy among infants of very low birthweight (<1500 g) or born prematurely (<32 weeks) in 16 European centres: a database study. Lancet 369, 43–50.

Rademaker, K.J., Lam, J.N., Van Haastert, I.C., Uiterwaal, C.S., Lieftink, A.F., Groenendaal, F., Grobbee, D.E., de Vries, L.S., 2004. Larger corpus callosum size with better motor performance in prematurely born children. Semin. Perinatol. 28 (4), 279–287 (Aug).

Reidy, N., Morgan, A., Thompson, D.K., Inder, T.E., Doyle, L.W., Anderson, P.J., 2013. Impaired language abilities and white matter abnormalities in children born very preterm and/or very low birth weight. J. Pediatr. 162 (4), 719–724 (Apr).

Reuter, M., Rosas, H.D., Fischl, B., 2010. Highly accurate inverse consistent registration: a robust approach. NeuroImage 53 (4), 1181–1196 (Dec).

Rimol, L.M., Nesvåg, R., Hagler Jr., D.J., Bergmann, O., Fennema-Notestine, C., Hartberg, C.B., Haukvik, U.K., Lange, E., Pung, C.J., Server, A., Melle, I., Andreassen, O.A., Agartz, I., Dale, A.M., 2012. Cortical volume, surface area, and thickness in schizophrenia and bipolar disorder. Biol. Psychiatry 71 (6), 552–560 (Mar 15).

Saygin, Z.M., Norton, E.S., Osher, D.E., Beach, S.D., Cyr, A.B., Ozernov-Palchik, O., Yendiki, A., Fischl, B., Gaab, N., Gabrieli, J.D., 2013. Tracking the roots of reading ability: white matter volume and integrity correlate with phonological awareness in prereading and early-reading kindergarten children. J. Neurosci. 33 (33), 13251–13258 (Aug 14).

Ségonne, F., Dale, A.M., Busa, E., Glessner, M., Salat, D., Hahn, H.K., Fischl, B., 2004. A hybrid approach to the skull stripping problem in MRI. NeuroImage 22 (3), 1060–1075 (Jul).

Ségonne, F., Pacheco, J., Fischl, B., 2007. Geometrically accurate topology-correction of cortical surfaces using nonseparating loops. IEEE Trans. Med. Imaging 26 (4), 518–529 (Apr).

Skranes, J., Vangberg, T.R., Kulseng, S., et al., 2007. Clinical findings and white matter abnormalities seen on diffusion tensor imaging in adolescents with very low birth weight. Brain 130, 654–666.

Skranes, J., Løhaugen, G.C., Martinussen, M., Håberg, A., Brubakk, A.M., Dale, A.M., 2013. Cortical surface area and IQ in very-low-birth-weight (VLBW) young adults. Cortex 49 (8), 2264–2271 (Sep).

Sled, J.G., Zijdenbos, A.P., Evans, A.C., 1998. A nonparametric method for automatic correction of intensity nonuniformity in MRI data. IEEE Trans. Med. Imaging 17 (1), 87–97 (Feb).

Smith, S.M., Jenkinson, M., Johansen-Berg, H., Rueckert, D., Nichols, T.E., Mackay, C.E., Watkins, K.E., Ciccarelli, O., Cader, M.Z., Matthews, P.M., Behrens, T.E., 2006. Tract-based spatial statistics: voxelwise analysis of multi-subject diffusion data. NeuroImage 31 (4), 1487–1505 (Jul 15).

Song, S.K., Yoshino, J., Le, T.Q., Lin, S.J., Sun, S.W., Cross, A.H., et al., 2005. Demyelination increases radial diffusivity in corpus callosum of mouse brain. NeuroImage 26, 132–140.

Spittle, A.J., Cheong, J., Doyle, L.W., Roberts, G., Lee, K.J., Lim, J., Hunt, R.W., Inder, T.E., Anderson, P.J., 2011. Neonatal white matter abnormality predicts childhood motor impairment in very preterm children. Dev. Med. Child Neurol. 53 (11), 1000–1006 (Nov).

Squeglia, L.M., Jacobus, J., Sorg, S.F., Jernigan, T.L., Tapert, S.F., 2013. Early adolescent cortical thinning is related to better neuropsychological performance. J. Int. Neuropsychol. Soc. 19 (9), 962–970 (Oct).

Staudt, M., Pavlova, M., Bohm, S., Grodd, W., Krageloh-Mann, I., 2003. Pyramidal tract damage correlates with motor dysfunction in bilateral periventricular leukomalacia (PVL). Neuropediatrics 34, 182–188.

Sullivan, M.C., Margaret, M.M., 2003. Perinatal morbidity, mild motor delay, and later school outcomes. Dev. Med. Child Neurol. 45, 104–112.

Tao, J.D., Neil, J.J., 2014. Advanced magnetic resonance imaging techniques in the preterm brain: methods and applications. Curr. Pediatr. Rev. 10 (1), 56–64.

Thiebaut de Schotten, M., Dell'Acqua, F., Forkel, S.J., Simmons, A., Vergani, F., Murphy, D.G., Catani, M., 2011. A lateralized brain network for visuospatial attention. Nat. Neurosci. 14 (10), 1245–1246 (Sep 18).

Thompson, D.K., Inder, T.E., Faggian, N., Warfield, S.K., Anderson, P.J., Doyle, L.W., Egan, G.F., 2012. Corpus callosum alterations in very preterm infants: perinatal correlates and 2 year neurodevelopmental outcomes. NeuroImage 59 (4), 3571–3581 (Feb 15).

Thompson, D.K., Thai, D., Kelly, C.E., Leemans, A., Tournier, J.D., Kean, M.J., Lee, K.J., Inder, T.E., Doyle, L.W., Anderson, P.J., Hunt, R.W., 2013. Alterations in the optic radiations of very preterm children—perinatal predictors and relationships with visual outcomes. Neuroimage Clin. 4, 145–153 (Nov 28).

Tzarouchi, L.C., Xydis, V., Zikou, A.K., Drougia, A., Astrakas, L.G., Papastefanaki, M., Andronikou, S., Argyropoulou, M.I., 2011. Diffuse periventricular leukomalacia in preterm children: assessment of grey matter changes by MRI. Pediatr. Radiol. 41 (12), 1545–1551 (Dec).

Van Braeckel, K., Butcher, P.R., Geuze, R.H., van Duijn, M.A., Bos, A.F., Bouma, A., 2010. Difference rather than delay in development of elementary visuomotor processes in children born preterm without cerebral palsy: a quasi-longitudinal study. Neuropsychology 24 (1), 90–100 (Jan).

van den Hout, B.M., de Vries, L.S., Meiners, L.C., et al., 2004. Visual perceptual impairment in children at 5 years of age with perinatal haemorrhagic or ischaemic brain damage in relation to cerebral magnetic resonance imaging. Brain Dev. 26, 251–261.

Vangberg, T.R., Skranes, J., Dale, A.M., Martinussen, M., Brubakk, A.M., Haraldseth, O., 2006. Changes in white matter diffusion anisotropy in adolescents born prematurely. NeuroImage 32 (4), 1538–1548 (Oct 1).

Vasung, L., Fischi-Gomez, E., Hüppi, P.S., 2013. Multimodality evaluation of the pediatric brain: DTI and its competitors. Pediatr. Radiol. 43 (1), 60–68 (Jan).

Vesia, M., Crawford, J.D., 2012. Specialization of reach function in human posterior parietal cortex. Exp. Brain Res. 221 (1), 1–18 (Aug).

Volpe, J.J., 2001. Neurobiology of periventricular leukomalacia in the premature infant. Pediatr. Res. 50, 553–562.

Volpe, J.J., 2009. Brain injury in premature infants: a complex amalgam of destructive and developmental disturbances. Lancet Neurol. 8 (1), 110–124 (Jan).

Wakana, S., Caprihan, A, Panzenboeck, M.M., Fallon, J.H., Perry, M, Gollub, R.L., Hua, K., Zhang, J., Jiang, H., Dubey, P., Blitz, A., van Zijl, P., Mori, S., 2007. Reproducibility of quantitative tractography methods applied to cerebral white matter. NeuroImage 36 (3), 630–644 (Jul 1).

Williams, J., Lee, K.J., Anderson, P.J., 2010. Prevalence of motor-skill impairment in preterm children who do not develop cerebral palsy: a systematic review. Dev. Med. Child Neurol. 52 (3), 232–237 (Mar).

Wolke, D., Sohne, B., Ohrt, B., Riegel, K., 1995. Follow-up of preterm children: important to document dropouts. Lancet 345, 447.